

Superconducting transport through a vibrating molecule

A. Zazunov,^{1,2} R. Egger,^{1,3} C. Mora,^{1,3} and T. Martin^{1,4}

¹ Centre de Physique Théorique, Case 907 Luminy, F-13288 Marseille cedex 9, France

² LPMMC CNRS, 25 av. des Martyrs, F-38042 Grenoble, France

³ Institut für Theoretische Physik, Heinrich-Heine-Universität, D-40225 Düsseldorf, Germany

⁴ Université de la Méditerranée, F-13288 Marseille cedex 9, France

(Dated: December 2, 2024)

Nonequilibrium electronic transport through a molecular level weakly coupled to a single coherent phonon/vibration mode has been studied for superconducting leads. The Keldysh Green function formalism is used to compute the current for the entire bias voltage range. In the subgap regime, Multiple Andreev Reflection (MAR) processes accompanied by phonon emission cause rich structure near the onset of MAR channels.

PACS numbers: 74.78.Na, 74.45.+c, 74.50.+r

One of the primary goals in the field of molecular electronics is to understand quantum transport through individual nanoscale objects, such as molecules, short carbon nanotubes, or DNA [1]. An important difference to conventional mesoscopic transport through quantum dots or granular islands arises because molecules can have intrinsic vibrational degrees of freedom ('phonons') that may give rise to Franck-Condon sidebands or phonon blockade in electronic transport [2, 3]. Molecular electronics is particularly exciting because it is in principle possible to contact molecules by leads of different nature. Here we discuss how nonequilibrium transport is affected by a coherent phonon mode coupled to the molecular charge for the case of (*s*-wave BCS) *superconducting leads*. Molecules connected to superconductors promise a rich terrain of exploration that allows for new spectroscopic tools (probing molecular properties), potentially useful applications, and interesting fundamental physics. First experimental results have appeared for carbon nanotubes [4] and metallocfullerenes [5].

So far transport through molecules has been theoretically studied only for normal leads, either using rate equations or (in the quantum-coherent regime) perturbation theory in the electron-phonon coupling λ [3]. For superconducting leads and large transmission through the molecule, subgap transport is ruled by MAR processes [6]. These have been extensively studied for point contacts [7] and for junctions containing a resonant level [8, 9]. In this paper, we provide a theoretical framework to include vibrations into superconducting transport through a resonant molecular level. We focus on the most interesting quantum-coherent low temperature (T) limit with high (bare) transmission, where Coulomb charging effects are largely wiped out. Therefore the Coulomb interaction on the molecule will be neglected here. We compute the d.c. current basically for the full bias (V) range within a Keldysh Green function scheme valid for small λ but arbitrary phonon frequency ω_0 . This approximation is current-conserving for identical molecule-lead couplings $\Gamma_L = \Gamma_R = \Gamma$ and superconductor gaps $\Delta_L = \Delta_R = \Delta$.

Our main results are as follows. (i) For $eV \gg \Delta$,

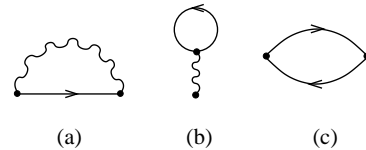


FIG. 1: Self energy due to the presence of the phonon mode: (a) 'Fock' and (b) 'tadpole' diagram. The polarization bubble (c) leads to the dressed phonon propagator \check{D} (wiggly lines). Arrowed lines denote \check{G}_0 .

the coupling λ tends to enhance the excess current I_{exc} , which is defined as the difference in current for $V \rightarrow \infty$ when changing normal into superconducting leads. (ii) In the subgap regime $eV < 2\Delta$, the phonon gives rise to a quite complicated structure in the I - V characteristics around each MAR onset at $eV = 2\Delta/n$ (integer n), with a pronounced even-odd parity dependence. These results can be qualitatively understood within a MAR ladder picture. Such a picture has previously been used for junctions with a resonant level [9] and is here extended to include single-phonon emission processes. Rich features in the I - V curve appear already for $eV \ll \hbar\omega_0$, in contrast to normal leads where phonon signatures (e.g. sidebands) emerge only at $eV \geq \hbar\omega_0$ [2, 3]. (iii) For $V = 0$, we give analytical results for the Josephson current in the adiabatic limit, $\hbar\omega_0 \ll \Delta \ll \Gamma$. We find a reduction (but no destruction) of the critical current and a changed current phase relation, in qualitative agreement with Ref. [10] where the limit $\Gamma \ll \Delta$ has been studied.

Next we discuss how to arrive at these conclusions (we often put $e = \hbar = 1$). Writing

$$H = \omega_0 b^\dagger b + \sum (\epsilon_0 + \lambda X) d_\sigma^\dagger d_\sigma + H_L + H_R + H_T, \quad (1)$$

we consider one relevant molecular level (fermion operator d_σ for spin $\sigma = \uparrow, \downarrow$) at energy ϵ_0 . Since the calculation of MAR dominated transport is already involved for $\lambda = 0$, a nontrivial current-conserving self-consistent approach covering the large transmission limit seems out of question. Below we instead proceed using a perturbation theory with the small expansion parameter λ/Γ . Under

such an approach, however, current conservation is only ensured for the electron-hole symmetric case [11], $\epsilon_0 = 0$, considered in what follows [12]. In Eq. (1) we take a linear coupling [2] between the molecular charge and the phonon displacement $X = b + b^\dagger$ (boson operator b). The leads are described by a pair of standard BCS Hamiltonians, $H_{L/R}$. Using the Nambu vector $d = (d_\uparrow, d_\downarrow^\dagger)^T$, the Pauli matrix σ_z in Nambu space, and $\Gamma = \pi\nu_0|t_0|^2$ for (normal) lead density of states ν_0 , the lead-molecule coupling is $H_T = t_0 \sum_{k,j=L/R=\pm} \Psi_{jk}^\dagger \sigma_z e^{\pm i\sigma_z V t/2} d + \text{h.c.}$, where the voltage V enters via the time-dependent phase. The lead fermions Ψ_{jk} can be traced out exactly because H is quadratic in these operators.

We then employ Keldysh Green functions, see, e.g., Ref. [13], for the d fermion, $\mathcal{G}_{\alpha\alpha'}^{ss'}(t, t')$, where α, α' ($s, s' = \pm$) are Nambu (Keldysh) indices, and $\mathcal{D}^{ss'}(t, t')$ for $X = b + b^\dagger$. We write $\check{\mathcal{G}}$ to indicate the Keldysh(-Nambu) structure. Denoting the respective functions for $\lambda = 0$ by $\check{\mathcal{G}}_0$ and $\check{\mathcal{D}}_0$, and using the approximate self energies in Fig. 1, the dressed Green functions follow from the Dyson equation; the 'tadpole' diagram does not contribute for $\epsilon_0 = 0$. We use the double Fourier representation

$$\check{\mathcal{G}}(t, t') = \sum_{n,m=-\infty}^{+\infty} \int_F \frac{d\omega}{2\pi} e^{-i\omega_n t + i\omega_m t'} \check{\mathcal{G}}_{nm}(\omega), \quad (2)$$

with $\omega_n = \omega + nV$ for ω within the fundamental domain $F \equiv [-V/2, V/2]$. Likewise, we represent all other Green functions and self energies. For fixed $\omega \in F$, the Dyson equations are then given by the matrix equations

$$\check{\mathcal{G}}_{0,nm}^{-1}(\omega) = \delta_{nm}\omega_n \check{\tau}_z - \Gamma \sum_j \check{\gamma}_{j,nm}(\omega) \quad (3)$$

$$\check{\mathcal{G}}^{-1} = \check{\mathcal{G}}_0^{-1} - \check{\Sigma}, \quad \check{\mathcal{D}}^{-1} = \check{\mathcal{D}}_0^{-1} - \check{\Pi}, \quad (4)$$

where the Pauli matrix $\check{\tau}_z$ acts in Keldysh space, and $\check{\mathcal{D}}_{0,nm}^{-1}(\omega) = \delta_{nm}(2\omega_0)^{-1}(\omega_n^2 - \omega_0^2)\check{\tau}_z$. The self energy $\check{\gamma}_{j=L/R=\pm,nm}(\omega)$ due to tracing out the respective lead is given by the Nambu matrix

$$\begin{pmatrix} \delta_{nm} \check{X}(\omega_n \mp V/2) & \delta_{m,n\mp 1} \check{Y}(\omega_n \mp V/2) \\ \delta_{m,n\pm 1} \check{Y}(\omega_n \pm V/2) & \delta_{nm} \check{X}(\omega_n \pm V/2) \end{pmatrix}$$

with Keldysh matrices $\check{Y}(\omega) = -\Delta \check{X}(\omega)/\omega$ and

$$\check{X}(\omega) = \begin{cases} -\frac{\omega}{\sqrt{\Delta^2 - \omega^2}} \check{\tau}_z, & |\omega| < \Delta \\ \frac{i|\omega|}{\sqrt{\omega^2 - \Delta^2}} \begin{pmatrix} 2f_\omega - 1 & -2f_\omega \\ 2f_{-\omega} & 2f_\omega - 1 \end{pmatrix}, & |\omega| > \Delta \end{cases}$$

where $f_\omega = 1/(1 + e^{\omega/k_B T})$. Figure 1 yields for the po-

larization $\check{\Pi}$ and the self energy $\check{\Sigma}$:

$$\begin{aligned} \check{\Pi}_{nm}^{ss'}(\omega) &= -i\lambda^2 \text{tr} \sum_{n'm'} \int_F \frac{d\omega'}{2\pi} (\check{\tau}_K \check{\mathcal{G}}_{0;n'm'}(\omega') \check{\tau}_K)^{ss'} \\ &\quad \times \check{\mathcal{G}}_{0;m'-m,n'-n}^{s's}(\omega' - \omega), \end{aligned} \quad (5)$$

$$\begin{aligned} \check{\Sigma}_{nm}^{ss'}(\omega) &= i\lambda^2 \sum_{n'm'} \int_F \frac{d\omega'}{2\pi} \mathcal{D}_{n-n',m-m'}^{ss'}(\omega - \omega') \\ &\quad \times (\check{\tau}_K \check{\mathcal{G}}_{0;n'm'}(\omega') \check{\tau}_K)^{ss'}, \end{aligned} \quad (6)$$

where 'tr' extends over Nambu space only and $\check{\tau}_K = \check{\tau}_z \sigma_z$. The current through the left/right junction then follows using the general relation

$$I_{L/R} = \mp 2\Gamma \text{Re} \sum_{nm} \int_F \frac{d\omega}{2\pi} \text{tr} [\sigma_z \check{\gamma}_{L/R,nm}(\omega) \check{\mathcal{G}}_{mn}(\omega)]^{+-}, \quad (7)$$

with the phonon contribution

$$\delta I_{ph} \equiv I(\lambda) - I(\lambda = 0). \quad (8)$$

Current conservation, $I_L = I_R \equiv I$, has been verified. Using Eq. (7), we evaluate the I - V characteristics for $\lambda = 0.15\Gamma$ (unless noted otherwise) and $k_B T/\Delta = 0.01$. We truncate the summations such that $|\omega_n| < \omega_c = 20\Delta$; further increase of the bandwidth ω_c did not change results. Once F is discretized (typically, $\delta\omega = 0.008\Delta$ was sufficient for convergence), the matrix inversions in Eqs. (3) and (4) are done for each $\omega \in F$ separately, involving matrix dimensions of the order ω_c/eV . For very small eV/Δ , this becomes quite costly, and we limit ourselves to $eV/\Delta > 0.15$. For $\lambda = 0$, our scheme reproduces the results of Refs. [7, 9]. For $\Delta = 0$, we recover results of Ref. [3] when applicable. As additional check, Green function sum rules [13] were verified. We have monitored the average phonon number and find $N_{ph} \lesssim 1$ for $\lambda/\Gamma = 0.15$. The phonon distribution function revealed renormalizations of the peak position away from ω_0 by a few percent.

Let us then turn to results for the I - V curve in the sub-gap regime, where MAR provides the dominant transport mechanism. In particular, for $2\Delta/(n+1) < eV < 2\Delta/n$ (n integer), there is a total number n of Andreev reflections for electrons or holes within the superconducting gap. The I - V curve for $\Gamma = 2\Delta$ and $\omega_0 = 0.2\Delta$ is given in Fig. 2, where δI_{ph} is always negative. Note that in this fully transmitting limit, the I - V curve for $\lambda = 0$ is smooth and does not exhibit the MAR 'cusps' encountered at lower transmission [7]. Phonons now restore such features near MAR onsets, with pronounced even-odd 'parity' effects: For even (odd) n , δI_{ph} shows valleys (peaks) around $eV = 2\Delta/n$. This is clearly seen in the left inset of Fig. 2 for n up to 12.

In order to achieve a physical understanding of the even-odd effect, it is useful to invoke a MAR ladder picture in energy space, see Fig. 3. Usually the scattering

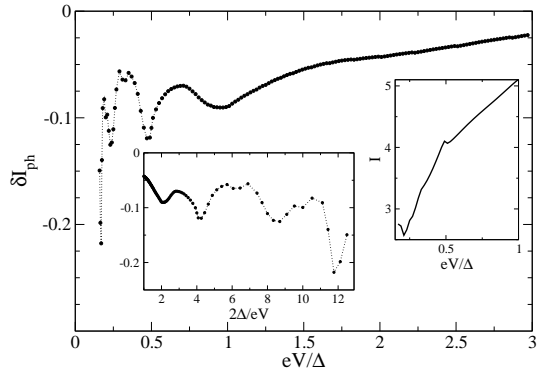


FIG. 2: Phonon difference current (8) for $\hbar\omega_0 = 0.2\Delta$ and $\Gamma = 2\Delta$. In all figures, currents are given in units of $e\Delta/(2\pi\hbar)$, and dotted lines are guides to the eye only. Left inset: Same as function of $2\Delta/eV$. Right inset: Part of the total I - V curve (note the scales).

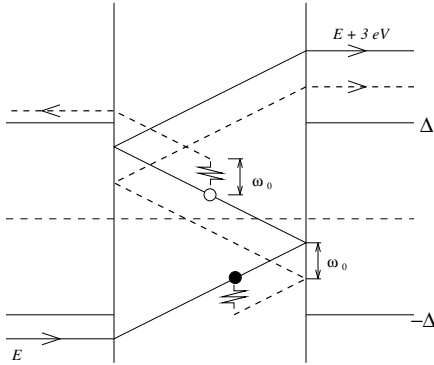


FIG. 3: MAR ladder picture with phonon emission. Here eV is slightly below Δ : for an electron incoming from the left side, we have one hole (open circle) and two electron (filled circle) segments. Dashed lines indicate possible trajectories after single phonon emission involving either hole or electron segments. There is also a MAR path (not shown) for a hole entering from the right side, with one electron and two hole segments.

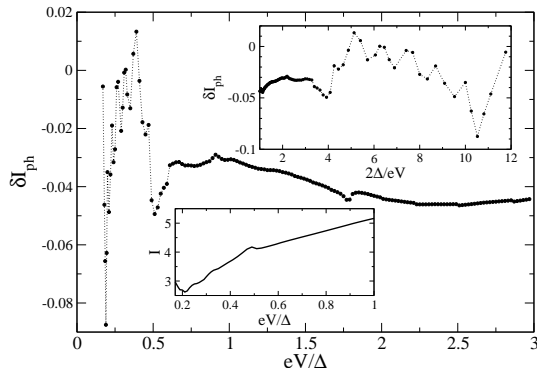


FIG. 4: Same as Fig. 2 but for $\hbar\omega_0 = 1.8\Delta$. The upper inset gives δI_{ph} as a function of $2\Delta/eV$, the lower inset gives the low-voltage part of the total current.

approach is used to develop this picture [9], but it encounters conceptual difficulties in the presence of inelastic phonon transitions. Fortunately, a different route resolving these difficulties can be formulated via the above Keldysh approach; for lack of space, details will be given elsewhere. Here 'bare' electron and hole propagators in energy space are coupled to each other through (i) the standard Andreev reflection self energy (mainly contributing in the subgap region) and (ii) the phonon self energy $\tilde{\Sigma}$. For a qualitative explanation of the even-odd effect found in the full calculation, cp. Fig. 2, it is sufficient to restrict the MAR ladder picture to *single* phonon emission processes, where electrons (holes) lose (gain) the energy $\hbar\omega_0$. Since $N_{ph} \lesssim 1$, emission dominates over absorption and multi-phonon processes are rare. In Fig. 3 the two superconductors are positioned at the same chemical potential, but electrons (from left to right) and holes (from right to left) 'climb' the MAR ladder by gaining eV for each Andreev reflection. The higher the total number of Andreev reflections in one cycle, the larger the total charge transmitted. Since we consider the high transmission limit (where high-order MAR processes are not penalized), the current is therefore expected to increase (decrease) if phonon emission is able to increase (decrease) the number of Andreev reflections in a MAR cycle. For eV slightly below $2\Delta/n$ with even n , we then argue as follows; for $n = 2$, see Fig. 3. For small energy transfer $\hbar\omega_0$, if a phonon is emitted during an electron segment, MAR trajectories in energy space are not drastically modified in the sense that the number of Andreev reflections stays unaffected. However, if a phonon transition occurs during a hole segment, the MAR ladder is shifted upwards by $\hbar\omega_0$ and the last hole on the MAR ladder can be scattered into the continuum (left electrode in Fig. 3) instead of being Andreev reflected. Consequently, one Andreev reflection is lost and hence the current is expected to decrease. This argument applies both to incoming electrons and holes, and explains why current valleys are observed for $eV \approx 2\Delta/n$ with even n in Fig. 2. On the other hand, consider eV slightly above $2\Delta/n$ with *odd* n . Reiterating the above analysis, now phonon emission during a hole segment tends not to affect the number of Andreev reflections. If the phonon is emitted during an electron segment, however, an additional Andreev reflection has to take place to complete the MAR cycle, leading to a current peak for $eV \approx 2\Delta/n$ with odd n .

Next consider $\hbar\omega_0 = 1.8\Delta$ but otherwise identical parameters, see Fig. 4, where δI_{ph} can be positive and again shows oscillations near the MAR onsets, which are less pronounced for small $n = 2\Delta/eV$. Remarkably, even for small voltages, $eV \ll \hbar\omega_0$, a rather complicated subgap structure is caused by the phonon. At such low voltages, this is only possible via MAR, for otherwise electrons or holes do not have enough energy to emit a phonon. The broad minimum corresponding to $n = 2$ observed in Fig. 2 has now vanished. Let us invoke the MAR ladder picture to rationalize this effect. For $eV \lesssim \Delta$,

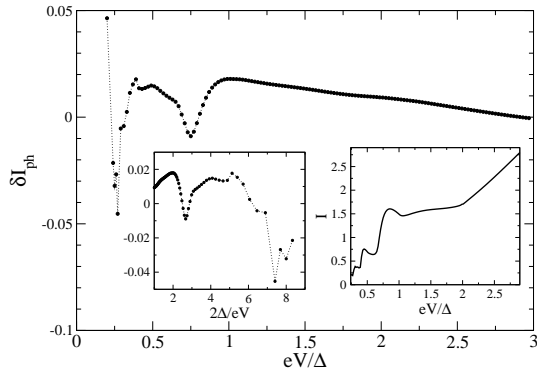


FIG. 5: Same as Fig. 2 but for $\Gamma = 0.5\Delta$. The left inset gives δI_{ph} versus $2\Delta/eV$, the right inset the total current.

by emitting a *high-energy* phonon ($\hbar\omega_0 > \Delta$), the last electron on the MAR ladder can now be scattered back inside the gap instead of heading to the continuum. This increases the number of reflections and thus the current. As a phonon emitted during the hole segment has the opposite effect (see above), the net outcome of the higher phonon frequency is to suppress the valley at $eV \approx \Delta$ expected for small ω_0 . Figure 4 also shows a dip in the current at $eV \approx 1.8\Delta$, representing a phonon backscattering feature at $eV = \hbar\omega_0$. The scaling of this dip with ω_0 was confirmed by additional calculations. One can also see a two-phonon feature at $eV = \hbar\omega_0/2$ in Fig. 4.

Let us then briefly go back to $\hbar\omega_0 = 0.2\Delta$ (cp. Fig. 2), but now for $\Gamma = 0.5\Delta$, see Fig. 5. For small Γ , quasi-resonances appear [9] and cause additional features, e.g. negative differential conductance portions in the I - V curve. The MAR ladder picture then has to include both quasi-resonances (cp. Ref. [9]) and phonon transitions, which is possible but beyond the scope of this paper. Fig. 5 shows that the even-odd parity effect

requires large Γ to be observable.

Finally, we discuss the limits of (i) very large or (ii) zero voltage. (i) We have computed the difference $\delta I_{exc,ph}$ between the excess currents I_{exc} with and without the phonon at $eV = 10\Delta$, which is large enough [9]. For our case of high transmission, we find that phonons generally *enhance* the excess current. To give a concrete example, for $\hbar\omega_0 = 0.8\Delta$, $\Gamma = 2\Delta$ and $\lambda = 0.5\Delta$, we find $\delta I_{exc,ph}/I_{exc} \approx 0.07$. A similar current enhancement at high transmission was also found for environmental Coulomb blockade in superconducting junctions, and has been explained as 'antiblockade' effect [14]. (ii) The equilibrium Josephson current has been calculated by adopting our approach to the Matsubara representation. The current phase relation in the adiabatic phonon regime $\hbar\omega_0 \ll \Delta \ll \Gamma$ is

$$I(\phi) = (e\Delta^2/2\hbar) T_0 \sin(\phi)/E_0(\phi), \quad (9)$$

where $E_0(\phi) = \Delta[1 - T_0 \sin^2(\phi/2)]^{1/2}$ is an Andreev bound state energy [7] in the junction with an effective transparency $T_0 = 1/(1 + \lambda^2/4\Gamma^2)$. The ϕ -dependent shift without any broadening of the Andreev level caused by the coupling to a phonon mode is characteristic for the coherent limit and decreases the critical current.

To conclude, we have explored molecular transport with superconducting leads in the coherent phonon regime. Phonons reveal a rich subgap structure even for voltages well below the phonon frequency, including an even-odd parity effect near the MAR onsets. Superconducting molecular transport surely warrants further theoretical and experimental surprises.

We thank V. Shumeiko for discussions. R.E. and C.M. are grateful to the CPT for hospitality. R.E. was supported by the CNRS and by the EU networks HYSWITCH and DIENOW.

[1] A. Nitzan and M.A. Ratner, *Science* **300**, 1384 (2003); G. Cuniberti, G. Fagas, and K. Richter (eds.), *Introducing Molecular Electronics*, Lect. Notes Phys. 680 (Springer 2005).

[2] D. Boese and H. Schoeller, *Europhys. Lett.* **54**, 668 (2001); S. Braig and K. Flensberg, *Phys. Rev. B* **68**, 205324 (2003); J. Koch and F. von Oppen, *Phys. Rev. Lett.* **94**, 206804 (2005).

[3] A. Mitra, I. Aleiner, and A.J. Millis, *Phys. Rev. B* **69**, 245302 (2004).

[4] M.R. Buitelaar, W. Belzig, T. Nussbaumer, B. Babic, C. Bruder, and C. Schönenberger, *Phys. Rev. Lett.* **91**, 057005 (2003); P. Jarillo-Herrero, J.A. van Dam, and L.P. Kouwenhoven, *Nature* **439**, 953 (2006); K. Grove-Rasmussen, H.I. Jorgensen, and P.E. Lindelof, cond-mat/0601371.

[5] A.Yu. Kasumov *et al.*, *Phys. Rev. B* **72**, 033414 (2005).

[6] T.M. Klapwijk, G.E. Blonder, and M. Tinkham, *Physica* (Amsterdam) **109B-110B**, 1657 (1982); G.B. Arnold, *J. Low Temp. Phys.* **68**, 1 (1987).

[7] E.N. Bratus, V.S. Shumeiko, and G. Wendin, *Phys. Rev. Lett.* **74**, 2110 (1995); D. Averin and A. Bardas, *Phys. Rev. Lett.* **75**, 1831 (1995); J.C. Cuevas, A. Martin-Rodero, and A.L. Yeyati, *Phys. Rev. B* **54**, 7366 (1996).

[8] A.L. Yeyati, J.C. Cuevas, A. López-Dávalos, and A. Martin-Rodero, *Phys. Rev. B* **55**, R6137 (1997).

[9] G. Johansson, E.N. Bratus, V.S. Shumeiko, and G. Wendin, *Phys. Rev. B* **60**, 1382 (1999).

[10] T. Novotny, A. Rossini, and K. Flensberg, *Phys. Rev. B* **72**, 224502 (2005).

[11] S. Hershfield, J.H. Davies, and J.W. Wilkins, *Phys. Rev. B* **46**, 7046 (1992); T. Frederiksen, M. Brandbyge, N. Lorente, and A.P. Jauho, *Phys. Rev. Lett.* **93**, 256601 (2004).

[12] This issue (and the tadpole diagram) was overlooked in Ref. [3], where the same approximation was implemented for normal leads but also used for the asymmetric case.

[13] A. Kamenev, in *Nanophysics: Coherence and Transport*

Les Houches session LXXXI, ed. by H. Bouchiat *et al.*
(Elsevier, 2005).

[14] A. Levy Yeyati, J.C. Cuevas, and A. Martin-Rodero,
Phys. Rev. Lett. **95**, 056804 (2005).